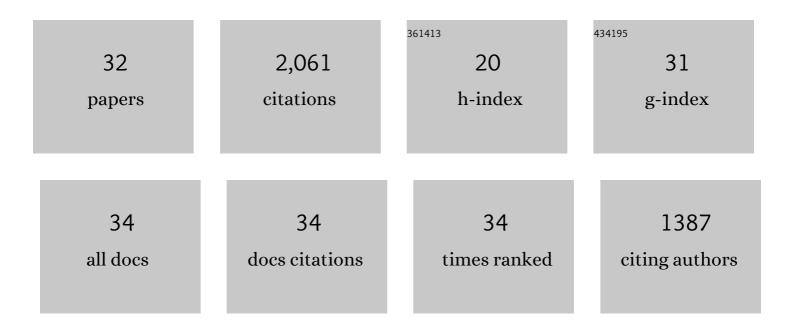
Zhaoshan Chang

List of Publications by Year in descending order

Source: https://exaly.com/author-pdf/11559556/publications.pdf Version: 2024-02-01



#	Article	IF	CITATIONS
1	U-Pb dating of zircon by LA-ICP-MS. Geochemistry, Geophysics, Geosystems, 2006, 7, n/a-n/a.	2.5	234
2	Geology of the post-collisional porphyry copper–molybdenum deposit at Qulong, Tibet. Ore Geology Reviews, 2009, 36, 133-159.	2.7	214
3	Exploration Tools for Linked Porphyry and Epithermal Deposits: Example from the Mankayan Intrusion-Centered Cu-Au District, Luzon, Philippines*. Economic Geology, 2011, 106, 1365-1398.	3.8	189
4	Sulfur isotopes in sediment-hosted orogenic gold deposits: Evidence for an early timing and a seawater sulfur source. Geology, 2008, 36, 971.	4.4	183
5	Age and pyrite Pb-isotopic composition of the giant Sukhoi Log sediment-hosted gold deposit, Russia. Geochimica Et Cosmochimica Acta, 2008, 72, 2377-2391.	3.9	151
6	The chlorite proximitor: A new tool for detecting porphyry ore deposits. Journal of Geochemical Exploration, 2015, 152, 10-26.	3.2	147
7	Regional Metallogeny of Mo-Bearing Deposits in Northeastern China, with New Re-Os Dates of Porphyry Mo Deposits in the Northern Xilamulun District. Economic Geology, 2016, 111, 1783-1798.	3.8	132
8	Zircon trace elements and magma fertility: insights from porphyry (-skarn) Mo deposits in NE China. Mineralium Deposita, 2019, 54, 645-656.	4.1	124
9	Composition and Evolution of Fluids Forming the Baiyinnuo'er Zn-Pb Skarn Deposit, Northeastern China: Insights from Laser Ablation ICP-MS Study of Fluid Inclusions*. Economic Geology, 2017, 112, 1441-1460.	3.8	93
10	Fluid compositions reveal fluid nature, metal deposition mechanisms, and mineralization potential: An example at the Haobugao Zn-Pb skarn, China. Geology, 2021, 49, 473-477.	4.4	79
11	Cospatial Eocene and Miocene granitoids from the Jiru Cu deposit in Tibet: Petrogenesis and implications for the formation of collisional and postcollisional porphyry Cu systems in continental collision zones. Lithos, 2016, 245, 243-257.	1.4	53
12	Spectral characteristics of propylitic alteration minerals as a vectoring tool for porphyry copper deposits. Journal of Geochemical Exploration, 2018, 184, 179-198.	3.2	53
13	The magmatic–hydrothermal transition—evidence from quartz phenocryst textures and endoskarn abundance in Cu–Zn skarns at the Empire Mine, Idaho, USA. Chemical Geology, 2004, 210, 149-171.	3.3	51
14	Using Mineral Chemistry to Aid Exploration: A Case Study from the Resolution Porphyry Cu-Mo Deposit, Arizona. Economic Geology, 2020, 115, 813-840.	3.8	48
15	Volcanic–plutonic connections and metal fertility of highly evolved magma systems: A case study from the Herberton Sn–W–Mo Mineral Field, Queensland, Australia. Earth and Planetary Science Letters, 2018, 486, 84-93.	4.4	39
16	Mineralogical Distribution of Germanium, Gallium and Indium at the Mt Carlton High-Sulfidation Epithermal Deposit, NE Australia, and Comparison with Similar Deposits Worldwide. Minerals (Basel,) Tj ETQq0 0	0 2g18T /Ov	ve do ck 10 Tf

17	Constraints on the ore fluids in the Chah Zard breccia-hosted epithermal Au–Ag deposit, Iran: Fluid inclusions and stable isotope studies. Ore Geology Reviews, 2015, 65, 512-521.	2.7	34
18	Age, igneous petrogenesis, and tectonic setting of the Bilihe gold deposit, China, and implications for regional metallogeny. Gondwana Research, 2016, 34, 296-314.	6.0	33

ZHAOSHAN CHANG

#	Article	IF	CITATIONS
19	The Louzidian Normal Fault near Chifeng, Inner Mongolia: Master Fault of a Quasi-Metamorphic Core Complex. International Geology Review, 2001, 43, 254-264.	2.1	32
20	Recent advances in the application of mineral chemistry to exploration for porphyry copper–gold–molybdenum deposits: detecting the geochemical fingerprints and footprints of hypogene mineralization and alteration. Geochemistry: Exploration, Environment, Analysis, 2020, 20, 176-188.	0.9	24
21	Intermediate sulfidation type base metal mineralization at Aliabad-Khanchy, Tarom-Hashtjin metallogenic belt, NW Iran. Ore Geology Reviews, 2018, 93, 1-18.	2.7	23
22	Timing and genesis of ore formation in the Qarachilar Cu-Mo-Au deposit, Ahar-Arasbaran metallogenic zone, NW Iran: Evidence from geology, fluid inclusions, O–S isotopes and Re–Os geochronology. Ore Geology Reviews, 2018, 102, 757-775.	2.7	16
23	The Paleozoic Mount Carlton Deposit, Bowen Basin, Northeast Australia: Shallow High-Sulfidation Epithermal Au-Ag-Cu Mineralization Formed During Rifting. Economic Geology, 2018, 113, 1733-1767.	3.8	13
24	Classifying Skarns and Quantifying Metasomatism at the Antamina Deposit, Peru: Insights from Whole-Rock Geochemistry. Economic Geology, 2020, 115, 177-188.	3.8	12
25	Geology and Genesis of the Cerro la Mina Porphyry-High Sulfidation Au (Cu-Mo) Prospect, Mexico. Economic Geology, 2017, 112, 799-827.	3.8	11
26	Delineating the structural controls on the genesis of iron oxide–Cu–Au deposits through implicit modelling: a case study from the E1 Group, Cloncurry District, Australia. Geological Society Special Publication, 2018, 453, 349-384.	1.3	9
27	Hyperspectral cathodoluminescence study of indium-bearing sphalerite from the Mt Carlton high-sulphidation epithermal deposit, Queensland, Australia. European Journal of Mineralogy, 2017, 29, 985-993.	1.3	8
28	Reconstruction of an Early Permian, Sublacustrine Magmatic-Hydrothermal System: Mount Carlton Epithermal Au-Ag-Cu Deposit, Northeastern Australia. Economic Geology, 2020, 115, 129-152.	3.8	6
29	The Watershed Tungsten Deposit, Northeast Queensland, Australia: Permian Metamorphic Tungsten Mineralization Overprinting Carboniferous Magmatic Tungsten. Economic Geology, 2021, 116, 427-451.	3.8	6
30	An Overview of <i>Mineral Deposits of China</i> . SEG Discovery, 2020, , 11-20.	1.0	6
31	INFLUENCE OF ORGANIC MATTER ON Re-Os DATING OF SULFIDES: INSIGHTS FROM THE GIANT JINDING SEDIMENT-HOSTED Zn-Pb DEPOSIT, CHINA. Economic Geology, 0, , .	3.8	1

Endoskarn and Cu-Zn mineralization at the Empire mine, Idaho, USA. , 2005, , 361-364.

0